

# Laboratory investigations of the role of the grain surface in astrochemical models

Wendy A. Brown,<sup>\*a</sup> Serena Viti,<sup>b</sup> Angela J. Wolff<sup>a</sup> and Amandeep S. Bolina<sup>a</sup>

Received 29th November 2005, Accepted 12th January 2006

First published as an Advance Article on the web 24th May 2006

DOI: 10.1039/b516770a

The rich chemistry often detected in star forming regions is now recognized to be a consequence of solid-state astrochemistry and the thermal desorption of its products. In recent experimental studies, desorption of a range of ices from a gold surface was investigated using temperature programmed desorption (TPD). These data were then used in astrochemical models. In this paper we investigate the sensitivity of these models to the inclusion of TPD data obtained from *different* surfaces (simulating different dust grains) and different thicknesses of the icy mantles. Detailed laboratory TPD studies of the desorption of ices from a highly oriented pyrolytic graphite (HOPG) surface have been performed. Desorption temperatures and kinetic parameters have been determined directly from the TPD data and have been used to determine the expected desorption temperature for the ices from grain surfaces. The results of these experiments have been incorporated into astrochemical models of high mass star forming regions and have then been compared with the results of previous experiments. From this comparison, we are able to determine whether the nature and composition of the grain surface is important in dictating the chemistry that occurs in star forming regions.

## Introduction

It has become clear that gas phase processes alone cannot account for the variety and richness of the chemistry observed in the interstellar medium, and in particular in dense regions of molecular clouds where star formation occurs. Instead, gas–grain interactions have been shown to play a key role in the chemistry of these environments.<sup>1</sup>

In star-forming regions, molecular ices are deposited on the surface of dust grains during the collapse of dense cores. Once the star is born ices evaporate and return to the gas phase. Before desorption occurs, however, the composition of the molecular ices often alters as they undergo surface reactions (mainly hydrogenation and oxidation) on the dust grains, and it is these surface reaction processes that give rise to the rich chemistry observed in these regions.

Desorption processes have been found to be particularly important in hot core regions.<sup>1,2</sup> Hot cores are small, dense, relatively warm, optically thick, and transient objects detected in the vicinity of newly formed massive stars. Hot cores exhibit a range of molecular species unlike those found in quiescent molecular clouds: in comparison, hot cores are richer in small saturated molecules and in large organic species.<sup>3</sup> Such richness arises due to the evaporation of processed ice, formed during the star formation process. In fact hot cores represent a late stage of star formation and in recent years there has been a wealth of observations that indicate the existence of possible precursors to hot cores<sup>4,5</sup> which should be chemically different from the hot cores themselves. Hence, molecular observations of hot cores, and their precursors, contain an integrated record of the physics of the collapse process during star formation.

Because massive stars form very rapidly, conventional studies of hot core chemistry always assume that desorption is instantaneous. However more recent studies<sup>6</sup> have shown that, in fact, the

<sup>a</sup> Department of Chemistry, University College London, 20 Gordon Street, London, UK WC1H 0AJ

<sup>b</sup> Department of Physics & Astronomy, University College London, Gower Street, London, UK WC1E 6BT

duration in which the dust is warmed from very low ( $\sim 10$  K) temperatures to the temperature typical of a hot core ( $\sim 300$  K) depends on the time taken for a pre-stellar core to evolve towards the so called Main Sequence. In turn, the time taken to evolve to the Main Sequence will depend on the final mass of the star. This suggests that it may be possible to determine the age of a hot core and its precursor, and hence the rise time of a star, from observations of molecular species in the gas phase during the desorption process. However, first, a thorough understanding of the desorption of icy mantles from grain surfaces must be obtained.

With this in mind, Collings *et al.* performed studies of the desorption of various astrophysically relevant molecules from a water ice surface deposited on a gold (Au) substrate held at 8–10 K. They performed investigations of the desorption of CO from a water ice surface<sup>7</sup> as well as detailed studies of the desorption of water<sup>8</sup> from the bare Au surface. In addition, the same authors have also undertaken a study of the desorption of a wide range of astrophysically relevant molecules both from a water ice surface, and from mixed ices deposited on Au, in an attempt to classify these molecules in terms of their desorption characteristics.<sup>9</sup> In this latter study, the intention was not to perform a detailed study of the desorption of all of the molecules, but rather was to give an indication of the way that each molecule behaves when desorbing from mixed ices adsorbed on interstellar grains. Detailed studies of the desorption of each molecule, such as those performed here, are therefore also necessary in order to obtain a full understanding of the desorption of molecular species from interstellar ices.

Collings and co-workers described four different types of desorption:<sup>9</sup> (1) monolayer desorption, where the molecule desorbs directly from the surface of the substrate or from the water ice; (2) multilayer desorption, where the desorbing species are present in sufficient quantities that they can form an outer layer, completely separated from the water; (3) volcano desorption, whereby so-called “trapped” molecules desorb as the water ice film undergoes a phase change from an amorphous structure to a crystalline structure; (4) and codesorption, whereby the trapped molecules are retained within the surface of the water until the crystalline water film desorbs. In practice, the four different types of desorption must correspond to different evolutionary stages observed during the formation of a star as they occur at different temperatures. Hence the common view that all ices are desorbed at once when the temperature reaches  $\sim 100$  K, or even that the ices evaporate with time according to their binding energy,<sup>6</sup> is incorrect. The investigated molecules were then separated into three categories, according to the observed characteristics of desorption. Water-like species showed only a single codesorption peak that was coincident with water desorption; CO-like species showed volcano and codesorption features, along with monolayer and multilayer desorption (at high doses); and intermediate species showed the volcano and codesorption peaks of trapped species, plus a small amount of monolayer desorption for molecules small enough to diffuse through the porous structure of amorphous water ice. The results of these models were then applied to the chemical modelling of massive star formation.<sup>2</sup> It was found that distinct chemical events, during desorption, occur at specific grain temperatures and that these differ depending on the mass of the star.<sup>2</sup> In particular, it was found that large species (including methanol) are good indicators of old cores as these strongly bound species are abundant only in the gas at late times. This implies that in the so called High Mass Protostellar Objects (or HMPOs), possibly the precursors of hot cores, we should not find the same chemical richness of organic species that is routinely found in hot cores. However, the species that were most affected by the inclusion of the new evaporation treatment were, not surprisingly, sulfur-bearing species. In fact while larger species such as methanol and  $\text{CH}_2\text{CO}$  maintain the same trends for stars with masses from 5 to 25 solar masses, the behaviour of sulfur bearing species strongly depends on the heating rate and hence on the mass of the star.

The previous experimental and modelling studies<sup>2</sup> showed how important it is to include reliable experimental data in astrochemical models. The next question to answer concerns the role that the type of surface plays in the adsorption and desorption of molecular ices on grains. In other words, it is important to investigate how sensitive astrochemical models are to the experimental set up, such as the composition of the simulated surface and the thickness of the simulated ices. This is particularly important since dust grains are composed of a range of materials, including siliceous and carbonaceous materials.

Evidence for the existence of carbon based dust grains suggests that these grains exist in the form of graphite, diamond or amorphous carbon.<sup>10,11</sup> Because of this, graphite is considered a good model grain surface and has been used for studies of the formation of small molecules on dust

grains.<sup>12–15</sup> In order to determine how the previous results<sup>2</sup> would differ if the experiments had been performed on graphite, rather than Au, we have undertaken detailed studies of the desorption of a range of ices from a highly oriented pyrolytic graphite (HOPG) surface held at 90 K. Although this temperature is not the same as that observed in the interstellar medium, where temperatures are usually around 10–20 K, it still allows a detailed understanding of the desorption of relevant species from HOPG to be gained. In fact, previous studies of the desorption of all of the species investigated here<sup>9</sup> have shown that desorption does not occur at temperatures below 100 K. Systems that we have investigated include the desorption of water from bare HOPG,<sup>16</sup> the desorption of methanol from bare HOPG<sup>17</sup> and from water surfaces of various thicknesses<sup>18</sup> and the desorption of mixed water/methanol ices from HOPG.<sup>18</sup> Here we compare the results of our detailed desorption studies with those of Collings and co-workers,<sup>2,9</sup> in order to gain an understanding of the role that the nature of the surface plays in the desorption of molecular ices from interstellar grains. The results of our investigations have been used in chemical models of massive star forming regions and, again, we compare the results obtained from these models with those previously obtained using experimental data determined by Collings and co-workers.<sup>2</sup> We have also investigated the role that the thickness of the ice plays in influencing the ice desorption temperature.

## Methodology

The experimental methods have been described in detail elsewhere.<sup>16,17</sup> Briefly, experiments were performed in an ultrahigh vacuum (UHV) chamber that has a base pressure of  $\leq 2 \times 10^{-10}$  mbar. The HOPG sample was purchased from Goodfellows Ltd. and was cleaved prior to installation in the chamber using the “Scotch tape” method.<sup>19</sup> The sample was cleaned before each experiment by annealing at 500 K in UHV for 3 min. The sample was cooled to 90 K and water (distilled, deionised water) and methanol (99.9% purity, BDH laboratory supplies Ltd) were admitted into the chamber by means of a high precision leak valve. The purity was checked with a quadrupole mass spectrometer before each experiment. Water/methanol mixed ices were dosed by mixing methanol and water in a glass bulb prior to dosing. The exact composition of the mixture formed was measured by recording a mass spectrum during the dosing process. All exposures are measured in Langmuir (L), where  $1 \text{ L} = 10^{-6}$  mbar s. TPD spectra were recorded with a Hiden Analytical HAL201 quadrupole mass spectrometer. All spectra were recorded at a heating rate of  $0.50 \pm 0.01 \text{ K s}^{-1}$ .

Data derived from the experiments were then incorporated into a chemical model. A complete description of this model can be found elsewhere.<sup>2</sup> Briefly, the model simulates the collapse of a cloud and follows the chemical evolution of the gas and dust during the collapse that ultimately leads to the formation of the star. The chemical network includes freeze out of the atoms and molecules onto the dust grains, as well as hydrogenation on the dust. After the collapse has been halted, the model follows the chemical evolution of the remnant cloud and how it is affected by the presence of the star. The presence of the star is simulated by subjecting the cloud to an increase in dust and gas temperature. Because it is relevant to the work described here, we will briefly summarize the way in which the temperature increases with time. The temperature reaches its maximum ( $\sim 300 \text{ K}$ ) at different contraction times depending on the mass of the new born star (see Table 2 of Viti *et al.*<sup>2</sup>). These times range from  $\sim 28\,000$  years for a 60 solar mass star to over a million years for a 5 solar mass star. During this time desorption occurs. The temperature was derived as a function of the luminosity (and therefore the age) of the protostar (see Viti *et al.*<sup>2</sup> for details). By correlating the temperature with age it was found that a power law fitted the observational data. Note, that the precise contraction time, and the exact behaviour of the temperature increase, are not important for this study as long as the contraction time of a massive protostar is comparable to the chemical timescale and as long as the temperature increases monotonically *i.e.* the temperature increase does not following a step function.

The evaporation treatment is pseudo-time dependent in that the evaporation of a fraction of mantle species  $X$  (in a single step) occurs when the temperature for a particular desorption event is reached. The desorption mechanism used is as previously used by Viti *et al.*<sup>2</sup> and therefore uses the classification of species derived in Collings *et al.*<sup>9</sup> as well as the volcano temperatures from their experiments. However, in the models presented in this paper, we have incorporated new results for the codesorption temperature of species desorbing from HOPG. We have also included a

reclassification of methanol from a water-like species (as indicated by Collings *et al.*<sup>9</sup>) to an intermediate species. Finally, we have also investigated the role that the ice thickness plays in determining the desorption of interstellar ices. Our results have been compared with results previously obtained by Viti *et al.* for the desorption of 0.3  $\mu\text{m}$  thick ices.<sup>2</sup>

## Results and discussion

### A: Experimental results

Fig. 1 shows TPD spectra recorded following the adsorption of a water/methanol mixture consisting of 8% methanol in water onto an HOPG surface held at 90 K (note, that in astronomical ices near massive stars solid methanol is believed to be  $\sim 1\text{--}10\%$  of the solid CO). The composition of the mixture was measured by using the mass spectrometer to measure the vapour pressure during dosing—this is not necessarily the composition of the resulting adsorbed ice. Our experiments show that, although the gas phase composition of methanol is approximately constant throughout the experiments shown in Fig. 1, the actual percentage of methanol in the ice mixture (determined by integrating the areas under the resulting water and methanol TPD peaks) varies quite dramatically, suggesting possible differences in the sticking probabilities of methanol and water on HOPG. Despite this observation, all effects were found to be constant for ice mixtures with a methanol percentage from 4–15%. The desorption of ices with thicknesses ranging from approximately  $5 \times 10^{-5}$  to  $5 \times 10^{-3} \mu\text{m}$  (corresponding to mixed water/methanol doses of 3–300 L) was investigated.

Fig. 1A shows spectra for the desorption of methanol from the HOPG surface and Fig. 1B shows spectra for the simultaneous desorption of water from the same surface. It is clear from Fig. 1A that only one desorption peak, at  $\sim 149$  K, is seen for methanol following low doses of the water/methanol mixture onto the HOPG surface. With increasing exposure this peak shifts up in

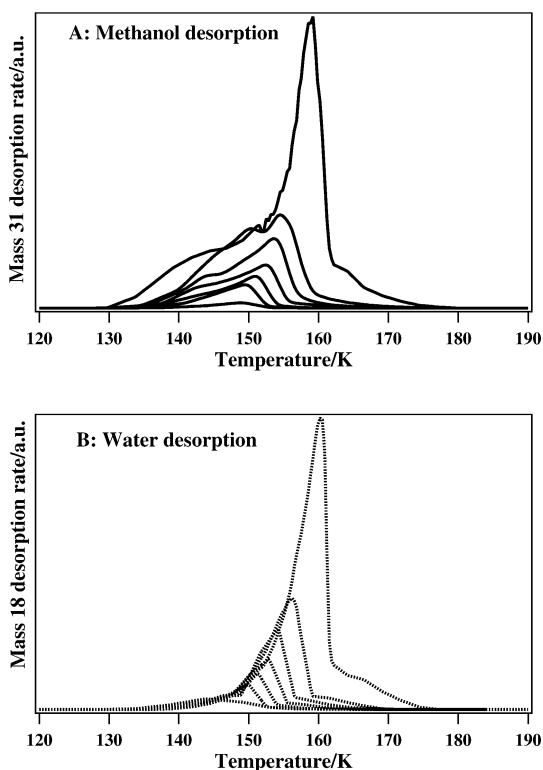


**Fig. 1** TPD spectra recorded following the adsorption of an 8% methanol in water mixture onto an HOPG sample held at 90 K. The spectra were recorded following doses of 3, 5, 7, 10, 15, 20 and 50 L of water/methanol mixture. (A) shows spectra for the desorption of methanol and (B) shows spectra for the desorption of water.

temperature, so that it has a desorption temperature of 158 K following the adsorption of a 50 L water/methanol mixture. A second, lower temperature, peak is also observed in the TPD spectra shown in Fig. 1A. This peak appears as a shoulder on the low temperature side of the main peak following adsorption of  $\geq 10$  L of the water/methanol mixture. With increasing dose of the water/methanol mixture, this peak becomes broader and more pronounced. Increasing the dose of the water/methanol mixture above 50 L does not lead to the observation of any additional desorption features in the TPD spectra. Instead, higher doses lead to spectra (not shown) in which the high temperature peak continues to increase in size and shift up in temperature, as well as becoming sharper. In contrast, the low temperature peak becomes much broader as the dose of water/methanol mixture is increased above 50 L.

Comparison of the TPD spectra recorded here for the desorption of methanol from mixed water/methanol ices adsorbed on HOPG with those previously recorded by Collings *et al.*<sup>9</sup> for the desorption of methanol from mixed ices adsorbed on Au show some differences. The data recorded here clearly show two peaks for methanol desorption (Fig. 1A), whereas Collings and co-workers<sup>9</sup> observed only one peak for the desorption of methanol. It is also clear from Fig. 1A that the desorption of methanol from mixed water/methanol ices is strongly coverage dependent. Collings *et al.*, however, did not investigate the coverage dependence of methanol desorption from mixed ices. This will be discussed in more detail later.

Spectra for the desorption of water from a mixed water/methanol ice adsorbed on HOPG at 90 K (Fig. 1B) show one main desorption feature at lower doses. This peak is initially observed at 145 K following a 3 L dose of mixed ice, and shifts up in temperature to reach 158 K following the adsorption of a 50 L water/methanol mixture. At higher doses of the mixture ( $\geq 20$  L) an additional, high temperature, peak is also observed. At the highest exposures shown in Fig. 1B (20 and 50 L), a further desorption feature is observed as a bump on the low temperature side of the main peak. This is shown more clearly in the 50 L spectrum, seen in Fig. 2. Increasing doses of the water/methanol mixture (not shown) do not lead to the observation of any additional features in the water TPD spectrum. However, the main peak and the high temperature peak continue to grow in intensity and shift up in temperature, whilst the low temperature shoulder becomes more pronounced with increasing dosage.

Assignments of the various desorbing species seen in the spectra in Fig. 1 can be made by comparison of these spectra with those recorded for the desorption of pure water<sup>16</sup> and pure methanol<sup>17</sup> from the HOPG surface. The spectra shown in Fig. 1B, for water desorption, are identical to those recorded following the adsorption of pure water on HOPG.<sup>16</sup> The main desorption feature in Fig. 1B is assigned to the desorption of multilayers of water. The assignment of this peak is confirmed by the observed increase in desorption temperature with increasing exposure and by the fact that the peak cannot be saturated. The low temperature bump that appears for higher water exposures (see Fig. 2) is assigned to the observation of an irreversible phase transition from amorphous solid water (ASW) to cubic crystalline ice (CI). Previous studies<sup>20–22</sup> have shown that water ice grows in the ASW phase at deposition temperatures below 135 K, with the exact morphology depending on the dosing conditions.<sup>23,24</sup> ASW has a glass transition temperature at  $\sim 135$  K,<sup>25,26</sup> above which it undergoes a phase transition to CI. The phase transition is accompanied by a change in the vapour pressure of the ice, and hence a change in the desorption rate, which manifests itself as a bump in the TPD spectrum. The observation of the phase transition means that the main water desorption peak, seen in Fig. 1B, is due to the desorption of crystalline water from the HOPG surface. The phase change from ASW to CI is initiated by the temperature ramp in the TPD experiment and occurs for all doses of the water/methanol mixture. However, as for pure water adsorbed on HOPG,<sup>16</sup> the characteristic bump in the TPD spectrum is only observed for thicker water/methanol ices. For thinner ices, conversion from ASW to CI occurs before desorption takes place. The additional, high temperature, water desorption peak seen in Fig. 1B following higher exposures of the water/methanol mixture can be assigned to a further phase transition from CI to hexagonal ice, in agreement with observations for pure water desorption from HOPG.<sup>16</sup>

Of relevance to astronomical ices, and in contrast to the water TPD spectra shown in Fig. 1B, methanol desorption from the mixed water/methanol ice layer is markedly different to methanol desorption from a pure methanol layer adsorbed on HOPG.<sup>17</sup> This suggests that the desorption of methanol is strongly influenced by the presence of water. Closer inspection of Fig. 1 shows that, in

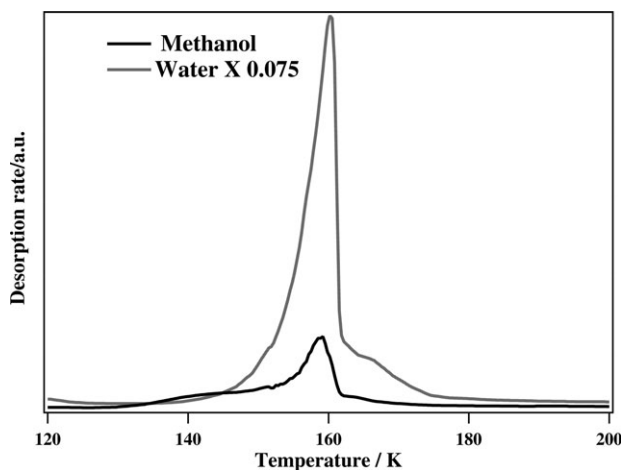


**Fig. 2** TPD spectra for the desorption of water and methanol from a mixed ice that results from the adsorption of a 50 L water/methanol mixture onto the HOPG surface at 90 K. The water spectrum has been scaled so that it appears on the same scale as the methanol.

fact, the main methanol desorption peak occurs in coincidence with the desorption of crystalline water. This is seen more clearly in Fig. 2, which shows an overlay of the methanol and water TPD spectra recorded following the adsorption of a 50 L mixed water/methanol layer on the HOPG surface at 90 K. Note that the water spectrum has been scaled to allow both spectra to be presented on the same graph. Overlays of the TPD spectra for other doses of the water/methanol mixture (not shown) also show similar effects. It is clear from Fig. 2 that the main methanol desorption occurs at the same temperature as the desorption of crystalline water, and hence this is assigned to a codesorption feature. The codesorbed methanol feature arises due to the desorption of methanol molecules that are trapped in the bulk of the water ice film and can only desorb when the water film also desorbs. The lower temperature methanol desorption feature can be assigned to a so called volcano desorption,<sup>9</sup> whereby trapped methanol molecules desorb from the surface as the water ice film undergoes a phase change from ASW to CI. This assignment is confirmed by the observation that the onset of this desorption feature occurs at 135 K, the temperature of the ASW to CI phase transition.<sup>25,26</sup> This peak becomes broader with increasing thickness of the mixed water/methanol ice layer due to the longer time it takes the thicker water layer to undergo crystallization.

As already discussed, Collings and co-workers observed only one desorption peak for methanol desorbing from mixed water/methanol ices. Hence they classified methanol as belonging to the water-like desorption category,<sup>9</sup> suggesting that only a codesorption peak should be observed. However, the data presented here clearly show the presence of both volcano and codesorption features, indicating that this classification is incorrect. We therefore suggest that methanol should, in fact, be classified as an intermediate species for desorption from interstellar ices. Collings and co-workers<sup>9</sup> previously showed that there are two types of intermediate species: those that show the desorption of monolayer species and those that do not. We have classified methanol as an intermediate species that does not show monolayer desorption. Note, however, that for methanol desorbing from the surface of a water ice film adsorbed on HOPG<sup>18</sup> monolayer desorption is also observed. If this monolayer adsorption were incorporated into the astronomical models, it is expected that the results observed would be different to those seen here. However, as it is expected that methanol in star forming regions exists in an intimate mixture with water ice, only results for mixed ices have been used in the models described here.

It is possible that the different categorisation of methanol in this study, compared to the study of Collings and co-workers,<sup>9</sup> is due to the use of different substrates in the two experiments. However, it is more likely that the fact that the experiments of Collings *et al.* were only performed for one dosage and for one percentage mixture means that they were unable to observe the full behaviour of the ice mixture and therefore were not able to categorise it correctly. Certainly, the only dosage that

they investigated was the adsorption of 100 L of mixed ice, whereas our investigations show that the volcano peak becomes much more pronounced for increasing doses of mixed ice up to 300 L. In fact, as already discussed, our results show that the TPD spectra for the desorption of mixed water/methanol ices show strong coverage dependence up to doses of around 50 L. This clearly demonstrates the importance of undertaking detailed studies of the desorption of astrochemically relevant molecules, in addition to the initial studies performed by Collings and co-workers.<sup>9</sup> Note, however, that it is the higher doses ( $\geq 50$  L) of mixed water/methanol ices that are most likely to be observed in star forming regions. Our results show that, for doses of mixed ice  $\geq 50$  L, the same two desorption features (a volcano peak and a codesorption peak) are always observed and that they shift up in temperature with increasing coverage. This observation is important, as astronomical ice thicknesses are believed not to be less than 0.02  $\mu\text{m}$  and are often assumed to be around 0.3  $\mu\text{m}$ <sup>27</sup>—much thicker than ices generally investigated in the laboratory. Hence in order to model ices of appropriate astronomical thicknesses, it is necessary to extrapolate laboratory data to larger thicknesses. It is clear from the data presented here that this is acceptable for mixed water/methanol ices since our results show that, for ice thicknesses greater than 50 L ( $10^{-3}$   $\mu\text{m}$ ), no additional desorption features are observed in the TPD spectrum.

The experimental results described here can be summarized as follows. Methanol has been categorized as an intermediate desorbing species (with no monolayer desorption) rather than as a water-like species as previously categorised by Collings and co-workers.<sup>9</sup> This recategorisation implies that a fraction of solid methanol may evaporate earlier in the evolution of the star formation process than previously thought.<sup>2</sup> Codesorption temperatures derived from the data shown in Fig. 1 (which varies with the mass of the star) are also different from those previously used<sup>2</sup> (see Table 1). Finally, we find that different ice thicknesses lead to different codesorption temperatures.

Table 1 shows the data incorporated into the astronomical models described here. Like the previous work,<sup>2</sup> we considered stars with masses ranging from 5 to 60 solar masses. From the experiments, we obtained the relevant codesorption temperatures and the fraction of the species desorbing in each of the observed desorption peaks (volcano, codesorption *etc.*). In Table 1 we also list the volcano temperatures (from previous experiments<sup>2</sup>) and the codesorption temperatures

**Table 1** Table showing the codesorption and volcano desorption temperatures, as a function of ice thickness, used in the astrochemical simulations described here. For all ice thicknesses, 76.5% of the methanol desorbed in the codesorption peak and 23.5% of the methanol desorbed in the volcano peak. Also included for comparison are the codesorption temperatures previously used by Viti and co-workers in an earlier model<sup>2</sup>

Star mass/ solar masses	Ice thickness/ $\mu\text{m}$	Volcano temperature <sup>2</sup> /K	Codesorption temperature/K	Previous codesorption temperature <sup>2</sup> /K
60	$1.1 \times 10^{-4}$	92.2	92.3	—
	$10^{-2}$	92.2	98.7	—
	0.3	92.2	104	103.4
	0.5	92.2	104.9	—
25	$1.1 \times 10^{-4}$	90.4	90.6	—
	$10^{-2}$	90.4	96.7	—
	0.3	90.4	101.8	101.6
	0.5	90.4	102.6	—
15	$1.1 \times 10^{-4}$	89.5	89.8	—
	$10^{-2}$	89.5	95.8	—
	0.3	89.5	100.8	100.8
	0.5	89.5	101.5	—
10	$1.1 \times 10^{-4}$	88.2	88.4	—
	$10^{-2}$	88.2	94.2	—
	0.3	88.2	99	99.4
	0.5	88.2	99.8	—
5	$1.1 \times 10^{-4}$	86.3	86.6	—
	$10^{-2}$	86.3	92.1	—
	0.3	86.3	96.7	97.5
	0.5	86.3	97.4	—

previously derived by Viti *et al.*<sup>2</sup> Table 1 also shows the way in which the thickness of the ice film affects the temperature of the codesorption feature. The way in which the data in Table 1 was obtained is described in the next section.

## B: Data for astronomical models

As already discussed, the data used in the models presented here differs from the data used previously by Viti and co-workers<sup>2</sup> in two ways. Firstly, as described above, methanol has been reclassified as an intermediate desorbing species, which gives rise to both volcano and codesorption features. The amount of methanol desorbing in each desorption feature was determined by peak fitting the TPD curves, obtained for methanol desorption, in order to separate the observed desorption into volcano desorption and codesorption. In TPD, the area under a curve is directly proportional to the amount of desorbing species. Hence it is possible to determine the proportion of methanol desorbing in the codesorption feature by plotting a graph of the total methanol integrated area against the integrated area of the codesorption peak. The gradient of this graph then gives the fraction of the methanol desorbing in the codesorption feature. Fig. 3 shows such a graph for a range of different TPD experiments, including those shown in Fig. 1, performed for various thicknesses of ices containing between 4 and 15% methanol in water. It is clear from Fig. 3 that the fraction of methanol desorbing in the codesorption feature is constant throughout this composition and thickness range. The gradient of the graph in Fig. 3 is 0.765. Hence, 76.5% of the methanol desorbs in the codesorption peak and 23.5% desorbs as a volcano desorption when the ASW to CI phase transition occurs.

The second way in which the models described here differ from the earlier models<sup>2</sup> is that, for some stellar masses, the codesorption temperature is different for the desorption of water from HOPG compared to water desorption from Au.<sup>9</sup> The codesorption temperature used in the astronomical models is evaluated by determining the kinetic parameters for water desorption and then using these parameters, along with an appropriate heating rate,<sup>2</sup> to determine the codesorption temperature for stars of different masses. The thermal desorption process, and hence the rate of desorption  $r_{\text{des}}$ , is described by the Polanyi–Wigner equation:<sup>28</sup>

$$r_{\text{des}} = A\theta^n \exp\left(\frac{-E_{\text{des}}}{RT}\right)$$

where  $A$  is the pre-exponential factor for the desorption process,  $\theta$  is the surface coverage of the desorbing species,  $n$  is the order of desorption,  $E_{\text{des}}$  is the activation energy for desorption,  $R$  is the gas constant and  $T$  is the surface temperature. Evaluating  $A$ ,  $n$  and  $E_{\text{des}}$  for a particular adsorbate system thus allows the simulation of TPD curves, and hence the determination of desorption

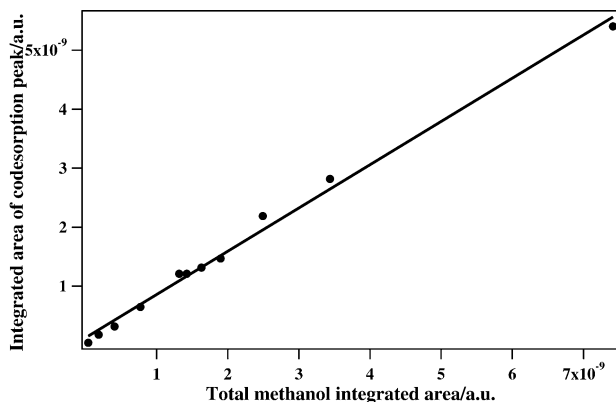


**Fig. 3** Graph showing the integrated area of the methanol codesorption peak as a function of the total integrated area of the methanol desorption for water/methanol ice mixtures composed of 4–15% methanol. The gradient of this graph gives the fraction of methanol that desorbs in coincidence with water desorption.

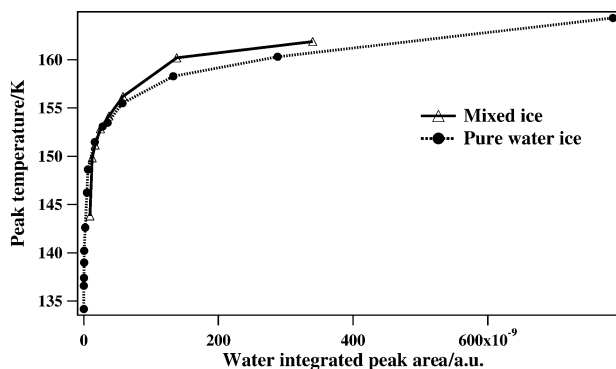


**Fig. 4** Graph showing the peak temperature of water desorption from pure water ice layers<sup>16</sup> and from mixed water/methanol ice layers adsorbed on HOPG, as a function of the total amount of adsorbed water (obtained from the total integrated area of the water desorption peak).

temperatures, for that particular adsorbate at any given initial surface coverage and for any heating rate.

The codesorption temperature used in the models described here was determined by evaluating kinetic parameters for the desorption of pure water from HOPG.<sup>16</sup> Comparison of the TPD data in Fig. 1 with data for the desorption of pure water from HOPG shows that the desorption temperature of water is unaffected by the presence of methanol. This is confirmed by Fig. 4, which shows a plot of the desorption temperature of pure water adsorbed on HOPG<sup>16</sup> and of water desorbing from mixed water/methanol ices adsorbed on HOPG. It is clear from Fig. 4 that the desorption temperature of water is the same for both adsorbate systems. Hence, using the kinetic parameters previously derived for pure water allows the determination of the codesorption peak temperature in mixed ices. Kinetic parameters for the desorption of water from HOPG have been determined,<sup>16</sup> and the values used to determine the codesorption peak temperature are shown in Table 2. The resulting codesorption peak temperatures for the desorption of various thicknesses of ice film are shown in Table 1 for stars of different masses.

### C: Results of astrochemical models

In the previous section we showed that TPD experiments on different surfaces and for different thicknesses of mixed ices, may lead to different desorption temperatures and also to different species classification. However, it is unclear, *a priori*, whether such differences are relevant to astrochemical models. For example, the differences in the codesorption temperatures derived here and those previously derived by Viti and co-workers<sup>2</sup> are generally just a few Kelvin-well within experimental and modelling errors (see Table 1). We have therefore used the data shown in Fig. 1 and Table 1 in astrochemical models of massive star forming regions to determine to what extent such models are sensitive to the conditions used in laboratory experiments. Testing the sensitivity of the models in this way is important, as it allows us to determine whether the nature of the grain surface has any effect or whether it is simply the presence of any surface that is important.

In order to compare directly with the astrochemical models in Viti *et al.*<sup>2</sup> we first ran the astrochemical models for ice thicknesses of 0.3  $\mu\text{m}$ . In the previous investigations<sup>2</sup> it was found that

**Table 2** Table showing the kinetic parameters for the desorption of water from HOPG,<sup>16</sup> used to determine the temperature of the codesorption peak

Parameter	
$n$	0.24
$E_{\text{des}}$	39.9 kJ mol <sup>-1</sup>
$A$	$1 \times 10^{27}$ molec m <sup>-2</sup> s <sup>-1</sup>

the two classes of species most affected by differential desorption are sulfur bearing species (such as  $\text{H}_2\text{S}$ ,  $\text{SO}$ ,  $\text{SO}_2$ ,  $\text{OCS}$ ) and large organic molecules (such as  $\text{CH}_3\text{OH}$ ,  $\text{CH}_2\text{CO}$ ,  $\text{HCOOCH}_3$ ). We therefore decided to concentrate on the differences that the changes described here may make to these species for stars of 5, 15, 25 and 60 solar masses. Note that the codesorption temperature for the 15 solar masses model is the same here as it was previously,<sup>2</sup> and hence any difference that we may find would be due to the different categorization of methanol. In fact the same occurs for the 25 solar masses model where, although the codesorption temperatures differ (see Table 1), the time at which the co-desorption occurs is the same. We can therefore use these two models to test the sensitivity to singular differences between the models.

For all masses, we find that sulfur bearing species are not affected by the different codesorption temperatures and different categorisation of methanol used in the present experiment. Hence we do not show here our comparison between the two models for sulfur bearing species. Large organic molecules, on the other hand, show some subtle differences but these are only important for low masses. Hence, in Fig. 5 we show the fractional abundances as a function of time for various large organic molecules. The figure compares the results of the present models (top panel) with the previous results from Viti *et al.*<sup>2</sup> (bottom panel) for a 5 solar mass star. In this figure, we can see that the different categorization of methanol leads to an earlier evaporation of methanol and to an earlier formation of  $\text{HCOOCH}_3$ . This occurs because  $\text{HCOOCH}_3$  is mainly formed in the gas phase *via* electronic recombination of the  $\text{H}_5\text{C}_2\text{O}_2^+$  ion, which in turn forms *via* the ion–neutral reaction of  $\text{H}_2\text{CO}$  with  $\text{CH}_3\text{OH}_2^+$ . The latter species then forms directly from methanol. Other species that are involved in reactions with methanol are water and OH, but these last two seem to be largely unaffected by the earlier evaporation of a fraction of the methanol (see Fig. 5). This is probably because all of the water evaporates at a later stage and OH is mainly formed *via* the dissociation of water. Note that, although such differences appear small, the difference in desorption timescales is as much as 30 000 years for methanol and  $\text{HCOOCH}_3$ . Hence this may be important in tracking the early stages of star formation.

Although the reclassification of methanol makes a difference for lower mass stars in general, however, we find that astrochemical models are not very sensitive to the differences between the

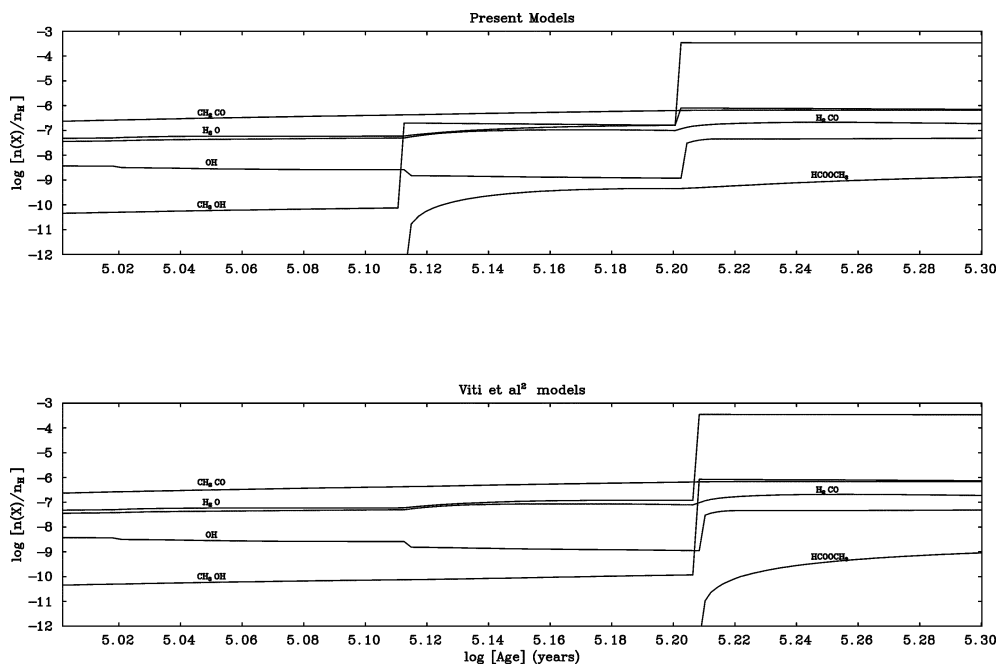


**Fig. 5** Fractional abundances of selected species as a function of time for a 5 solar mass star, equivalent to a contraction time of  $1.15 \times 10^6$  years, for the present model (top panel) compared to the previous Viti *et al.*<sup>2</sup> models (bottom panel).

experiments reported here for desorption from HOPG and the previous experiments for desorption from Au. In particular, the change in the codesorption temperature of a few Kelvin (see Table 1) does not affect the results of the astrochemical models. This is an extremely important result because it implies that the type of surface used for a particular experiment is of secondary importance to the actual presence of a surface. The most likely reason that the nature of the surface does not apparently affect the desorption of the ice species is because the species are physisorbed onto the surface and therefore not forming a chemical bond to the surface. In fact, our results suggest that icy mantles seem to desorb in the same manner regardless of the substrate. Of course we cannot say whether icy mantles on silicates would behave in the same manner as those on graphite and Au, but the fact that the use of one instead of the other did not make any substantial difference indicates that this may be the same for silicates. Note that the experimental investigations described here have only looked at the desorption of methanol and in order to be certain that the nature of the surface does not affect the observed desorption, it will also be necessary to perform detailed investigations of other astronomically relevant molecules.

We now briefly comment on how the thickness of the icy mantles may affect the differential desorption. As explained above, the experiments were performed for a variety of thicknesses ranging from around  $5 \times 10^{-5}$  to  $5 \times 10^{-3}$   $\mu\text{m}$ . These results were then extrapolated to give codesorption temperatures for ices with thicknesses of up to 0.5  $\mu\text{m}$ . The astrochemical models were then run for ices with thicknesses of  $1.1 \times 10^{-4}$ ,  $10^{-2}$ , 0.3 and 0.5  $\mu\text{m}$ , as seen in Table 1. The models showed that the desorption behaviour of all of the molecules studied (sulfur containing species and larger organics) does not vary significantly for ice thicknesses larger than  $10^{-3}$   $\mu\text{m}$ , and that most of the striking differences are observed for ice thicknesses between  $10^{-4}$  and  $10^{-3}$   $\mu\text{m}$ . In astronomical environments the ices are believed to be no less than 0.05  $\mu\text{m}$  in thickness, so again we conclude that as long as the experiments are performed with an icy mantle that has at least a thickness of  $10^{-3}$   $\mu\text{m}$ , then the desorption behaviour should not be sensitive to the adopted thickness, at least in the conditions used in the model presented here.

## Conclusions

In this paper we have presented new results for the desorption of mixed water/methanol ices from an HOPG surface. These results have been used to investigate the effect of the nature of the surface on the results of astrochemical models. In previous experiments on a Au surface, methanol was classified as a water-like species.<sup>9</sup> Here we find instead that methanol desorbs as an intermediate species (with no monolayer desorption). We also find that the codesorption temperature is different for ices desorbing from HOPG, compared to ices desorbing from a Au surface<sup>9</sup> and that the ice thickness affects the codesorption temperature. In order to test whether such differences are relevant in the interpretation of astronomical observations, we have used these results in astrochemical models of massive star forming regions, in the same manner as in Viti *et al.*<sup>2</sup> We find that the astrochemical models are *not* sensitive to the change in codesorption temperature, although methanol and  $\text{HCOOCH}_3$  behave differently for low mass stars due to the different classification of methanol. On the whole, these results imply that the nature of the surface is not important, but rather that it is simply the presence of any grain surface that matters. However, we believe that this is only the case for physisorbed species such as water and methanol.

## Acknowledgements

The EPSRC are thanked for studentships for ASB and AJW and for an equipment and consumables grant for the experiments. SV acknowledges the financial support of an individual PPARC advanced fellowship. Mark Wilson is thanked for his help in calculating the codesorption temperatures for use in the models.

## References

- 1 D. A. Williams, *Faraday Discuss.*, 1998, **109**, 1.
- 2 S. Viti, M. P. Collings, J. W. Deaver, M. R. S. McCoustra and D. A. Williams, *Mon. Not. R. Astron. Soc.*, 2004, **354**, 1141.

- 
- 3 C. M. Walmsley and P. Schilke, in *Dust and Chemistry in Astronomy*, ed. T. J. Millar and D. A. Williams, Institute of Physics Publishing, Bristol, 1993.
  - 4 H. Beuther, P. Schilke, K. M. Menten, F. Motte, T. K. Sridharan and F. Wyrowski, *Astrophys. J.*, 2002, **566**, 945.
  - 5 S. Molinari, L. Testi, L. F. Rodriguez and Q. Zahang, *Astrophys. J.*, 2002, **570**, 758.
  - 6 S. Viti and D. A. Williams, *Mon. Not. R. Astron. Soc.*, 1999, **305**, 755.
  - 7 M. P. Collings, J. W. Dever, H. J. Fraser and M. R. S. McCoustra, *Astrophys. Space Sci.*, 2003, **285**, 633.
  - 8 H. J. Fraser, M. P. Collings, M. R. S. McCoustra and D. A. Williams, *Mon. Not. R. Astron. Soc.*, 2001, **327**, 1165.
  - 9 M. P. Collings, M. A. Anderson, R. Chen, J. W. Dever, S. Viti, D. A. Williams and M. R. S. McCoustra, *Mon. Not. R. Astron. Soc.*, 2004, **354**, 1133.
  - 10 B. T. Draine, *Astrophys. J.*, 1988, **333**, 848.
  - 11 J. S. Mathis and G. Whiffen, *Astrophys. J.*, 1989, **341**, 808.
  - 12 J. S. A. Perry, J. M. Gingell, K. A. Newson, J. To, N. Watanabe and S. D. Price, *Meas. Sci. Technol.*, 2002, **13**, 1414.
  - 13 J. S. A. Perry and S. D. Price, *Astrophys. Space Sci.*, 2003, **285**, 769.
  - 14 V. Pirronello, C. Liu, J. E. Roser and G. Vidalai, *Astron. Astrophys.*, 1999, **344**, 681.
  - 15 N. Katz, I. Furman, O. Biham, V. Pirronello and G. Vidalai, *Astrophys. J.*, 1999, **522**, 305.
  - 16 A. S. Bolina, A. J. Wolff and W. A. Brown, *J. Phys. Chem. B*, 2005, **109**, 16836.
  - 17 A. S. Bolina, A. J. Wolff and W. A. Brown, *J. Chem. Phys.*, 2005, **122**, 044713.
  - 18 A. J. Wolff, C. Carlstedt and W. A. Brown, in preparation.
  - 19 R. Wiesendanger, L. Eng, H. R. Hidber, P. Oelhafen, L. Rosenthaler, U. Staufer and H. J. Guntherodt, *Surf. Sci.*, 1987, **189**, 24.
  - 20 G. P. Johari, A. Hallbrucker and E. Mayer, *J. Chem. Phys.*, 1991, **95**, 2955.
  - 21 P. Jenniskens and D. F. Blake, *Science*, 1994, **265**, 753.
  - 22 R. S. Smith, C. Huang, E. K. L. Wong and B. D. Kay, *Surf. Sci.*, 1996, **367**, L13.
  - 23 K. P. Stevenson, G. A. Kimmel, Z. Dohnalek, R. S. Smith and B. D. Kay, *Science*, 1999, **283**, 1505.
  - 24 E. Mayer and R. Pletzer, *Nature*, 1986, **319**, 298.
  - 25 Y. P. Handa and D. D. Klug, *J. Phys. Chem.*, 1988, **92**, 3323.
  - 26 A. Hallbrucker, E. Mayer and G. P. Johari, *J. Phys. Chem.*, 1989, **93**, 4986.
  - 27 D. C. B. Whittet, in *Dust in the Galactic Environment*, ed. R. J. Tayler and R. E. White, Institute of Physics Publishing, Bristol, 1992.
  - 28 A. M. de Jong and J. W. Niemantsverdriet, *Surf. Sci.*, 1990, **233**, 355.